

Edge-Density-Profile Effects for Lower-Hybrid-Waveguide Coupling

J. Stevens, M. Ono, R. Horton, and J. R. Wilson

Plasma Physics Laboratory, Princeton University
Princeton, New Jersey 08544

ABSTRACT

The usual predictions of linear coupling theory for lower hybrid waves are altered by including an overdense edge plasma ($\omega < \omega_{pe}$) in the plasma model. Coupling is found to depend strongly on the value of the edge density, as well as the density gradient. The regimes, where one or the other of these parameters is important, are investigated. Typically, only the first few millimeters of the edge plasma is important in determining coupling. The major implications of the problem of coupling to an overdense plasma can be derived from a simple impedance matching argument. In general, coupling is optimum for an edge density, n_0 , determined by $n_0/n_c \approx n_{\parallel}^2$, where $n_c = \omega^2 m_e / 4\pi e^2$ and n_{\parallel} is the parallel index of refraction of the lower hybrid wave.

DISCLAIMER



I. Introduction

Lower hybrid wave heating of thermonuclear plasmas has the advantage of using simple phased waveguide arrays [1]. These arrays couple naturally to the plasma without matching elements. Previous linear coupling calculations [2-7] have been done by assuming a plasma model consisting of a density ramp beginning at zero density at the plasma edge, with a vacuum region separating the plasma from the coupler aperture in some cases (Fig. 1, curve A). While such a plasma model adequately describes some experimental situations, it is not valid for tokamak experiments in general. In particular, it is likely that the plasma density near the waveguide aperture greatly exceeds the critical density, defined by $n_c = \omega^2 m_e / 4\pi e^2$. We find that the coupling properties of lower hybrid waves depend strongly on the absolute density which occurs at, or very near, the waveguide aperture. In this paper, we will investigate the effects of the plasma edge density on the coupling of lower hybrid waves.

To choose a plasma model, we note that a coupling structure only perturbs the plasma locally in the direction perpendicular to the magnetic field. Thus, the density will increase from zero to its unperturbed value in a short distance from the structure, beyond which it maintains the same density gradient as in the unperturbed case. Measurements in Princeton's PLT machine show edge densities larger than n_c (for $\omega/2\pi = 800$ MHz)

behind the limiter [8], at the expected position of the waveguide aperture. Thus, provided the density beyond the aperture is not affected much by the coupler, it is reasonable to model the plasma edge profile as a density step plus a density ramp (Fig. 1, curve B). Several authors have recently proposed such models for the edge plasma [9-11] in connection with nonlinear lower hybrid wave coupling, but the implications to the linear coupling problem were not studied in detail.

In this paper, we numerically solve the linear waveguide coupling problem for the step + ramp model of the plasma edge density. These calculations are done using computer codes with the flexibility to treat arbitrary density profiles. An analytic formula is derived which explains the major features of the numerical results. Finally, the regimes of validity for the step + ramp model are explored.

II. Numerical Methods

Two independent computer codes were used to study lower hybrid wave coupling. Both differ from the usual formulation² in the model of the edge plasma density profile. Higher order waveguide modes were also neglected in both codes for this study. Curve A in Fig. 1 shows the ramp profile model used by most previous authors [2-7]. The coupler aperture is at $x = 0$, n_c is the cut-off density where $\omega = \omega_{pe}$, and n_1 , x_1 , and n_0 are

defined by the figure. The ramp profile model can easily be extended to include a density step plus a density ramp. This profile is shown as curve B in Figure 1, and defined by

$$n(x) = [n_0 + \nabla n (x-x_0)] u(x-x_0) \quad (1)$$

where n_0 is the density step, x is the distance normal to the plasma surface, x_0 is the distance from the plasma to the coupler (usually $x_0 = 0$), and $u(x-x_0)$ is the unit step function. This model has been used previously in the study of ponderomotive effects [10], and will be valid provided the step in density from 0 to n_0 is sharp enough. The resulting normalized plasma impedance is given by

$$\begin{aligned} z(n_{\parallel}) &= \frac{|n_{\perp}|^{1/3}}{(\nabla n/n_c)^{1/3}} \frac{\text{Ai}(W_0) + i \text{Bi}(W_0)}{\text{Ai}'(W_0) + i \text{Bi}'(W_0)}, \quad |n_{\parallel}| > 1 \\ &= \frac{i |n_{\perp}|^{1/3}}{(\nabla n/n_c)^{1/3}} \frac{\text{Ai}(W_0)}{\text{Ai}'(W_0)}, \quad |n_{\parallel}| < 1 \end{aligned} \quad (2)$$

where Ai and Bi are Airy functions, n_{\parallel} is the parallel index of refraction, $n_{\perp} = (1-n_{\parallel}^2)^{1/2}$, and

$$W_0 = \frac{-(n_{\parallel}^2 - 1)^{1/3}}{(\nabla n/n_c)^{1/3}} \left(\frac{n_0}{n_c} - 1 \right). \quad (3)$$

The ramp model studied by Brambilla [1] takes $W_0 = 0$, i.e., $n_0 = n_c$.

A second computer code models the plasma as an arbitrary number of density steps, allowing more complicated plasma profiles to be studied by appropriately choosing the number of steps[9]. Here we shall mainly use this code to establish the region of importance and the range of validity for the simplified plasma models as shown in Fig. 1. Both codes duplicate the Brambilla results [2] when a linear ramp model is used.

III. Results

The grill designed for the Princeton PLT experiment will be used to demonstrate the effect of the step + ramp plasma profile model on lower hybrid wave coupling. RF power at 800 MHz is supplied to six waveguides of width 3.5 cm, each separated by a 0.63 cm septum. The density profile in front of the coupler is given by curve B in Fig. 1.

The total reflected power (R) for the six waveguide grill is plotted versus n_o/n_c in Fig. 2, for density gradients of 10^{10} to 10^{13} cm^{-4} and a relative phasing between waveguides of $\Delta\phi = \pi$. The ramp model ($n_o/n_c = 1$) is sensitive to ∇n , but n_o/n_c becomes an important factor determining coupling for an overdense ($n_o > n_c$) plasma at the coupler aperture. It is apparent, from the figure, that there is an optimum edge density at which coupling is best. Also note that coupling

to an overdense plasma can be more efficient than coupling into a ramping density profile.

The total reflected power versus n_o/n_c is shown in Fig. 3, for $\nabla n = 10^{11} \text{ cm}^{-4}$ and relative phasings between guides of $0, \pi/4, \pi/2, 3\pi/4,$ and π . This demonstrates that the edge density for optimum coupling decreases as $n_{||}$ decreases.

The reflected power in the individual waveguides versus n_o/n_c is shown in Fig. 4 for $\nabla n = 10^{11} \text{ cm}^{-4}$ and $\Delta\phi = \pi$. It is seen that the relative reflected powers in the individual guides change as a function of n_o/n_c . For instance, the outside guides couple best when $n_o/n_c = 1$ (ramp model) while the inside guides couple best when $n_o/n_c > 20$.

The $n_{||}$ power spectrum in the plasma is shown in Fig. 5, for $n_o/n_c = 1, 20,$ and 400 . $\nabla n = 10^{11} \text{ cm}^{-4}$ and relative phasing between waveguides of π . The part of the spectrum near $n_{||} = 1.0$ is highest for the case of $n_o/n_c = 1$ and lowest for $n_o/n_c = 400$. Near $n_{||} = 4.5$, the power spectrum is highest for the case of $n_o/n_c = 20$.

All of the above results can be explained by considering the simple example of coupling to a uniform overdense plasma (i.e., curve B, Fig. 1 in the limit of zero density gradient). The Fourier transformed axial electric field for lower hybrid waves in the plasma is given by the solution of

$$\frac{\partial^2 E_z(x, n_{||})}{\partial x^2} + (n_{||}^2 - 1) \left(\frac{n_o}{n_c} - 1 \right) E_z(x, n_{||}) = 0, \quad (4)$$

where x is the direction normal to the plasma surface, z is parallel to the external magnetic field, and all distances are normalized by the free space wavenumber $k_0 = \omega_0/c$. Matching plasma and waveguide solutions at the plasma edge in the usual manner [2] gives a plasma reflection coefficient (for $|n_n| > 1$) of

$$\rho(n_n) = \frac{Z - 1}{Z + 1}, \quad (5)$$

where

$$Z(n_n) = \frac{(n_n^2 - 1)^{1/2} (1 - (\pi/k_0 a)^2)^{1/2}}{(n_0/n_c - 1)^{1/2}} \quad (6)$$

is the plasma impedance normalized to the waveguide impedance (TE₁₀ mode). We neglect the effect of waveguide height for the remainder of this paper, i.e., $a \rightarrow \infty$ and $(1 - (\pi/k_0 a)^2)^{1/2} \rightarrow 1$. The least reflection occurs when $|Z| = 1$, giving the condition for optimum coupling as

$$\frac{n_0}{n_c} = n_n^2. \quad (7)$$

The plasma impedance given by Eq. (6) is real while the impedance derived from the ramp model [2,12] has an imaginary component:

$$Z_{\text{ramp}}(n_n) = \frac{1.37 |n_n|^{1/3} e^{-\pi i/3}}{(n/n_c)^{1/3}} \quad (|n_n| > 1). \quad (8)$$

The step + ramp model will have a reactive component of impedance somewhere between the extremes given by Eqs. (6) and (8).

Less of a reactive component means that coupling into an overdense plasma can be more efficient. The cases shown in Figs. 2-5 and all other cases studied show the expected optimum coupling at $n_o/n_c \approx n_u^2$. For instance, the main peak of the spectrum for the case shown in Figs. 3-5 is at $n_u = 4.5$ for $\Delta\phi = \pi$ and the optimum coupling is at $n_o/n_c \approx 4.5^2 \approx 20$. For $\Delta\phi = \pi/2$, $n_u \approx 2.25$ and $n_o/n_c \approx 5$ for best coupling. The reason that the outside guides in Fig. 4 couple best at low n_o/n_c is that they have neighboring guides on only one side. Thus, they act partially like a single waveguide which couples best at longer wavelengths[13] (low n_u). The interior guides have neighboring guides on each side and couple best at the higher n_u determined by the π phasing. Thus, they approach their optimum coupling at higher n_o/n_c .

The question of whether the conditions for the step + ramp profile model are possible experimentally will now be considered. For a coupler pushed into the plasma, the density increases from zero at the waveguide aperture to n_o in a distance of the order of the sheath thickness. The model density profile shown by curve C in Fig. 1 was chosen to investigate the effect of the sheath thickness. The density profile ramps from $n = n_c$ at $x \approx 0$ to $n = n_1$ at $x = x_1$, beyond which it remains constant. Reflection R is plotted in Fig. 6 as a function of distance x_1 , with n_1/n_c held at

certain fixed values while V_n is allowed to vary. The distance X_1 thus simulates the sheath thickness. Values of n_1/n_c of 10, 100, and 1000, and relative waveguide phasings of $\pi/2$ and π are shown in Fig. 6. It is seen that below a certain X_1 ($\equiv X_1^*$) the reflected power is independent of X_1 . The distance X_1^* , beyond which the reflected power changes, decreases with higher n_1/n_c and also decreases with higher n_n . The explanation for this result is that the ramp width X_1 , i.e., sheath thickness, is not important so long as it is less than a small fraction of the perpendicular wavelength, given by

$$\lambda_{\perp}(x) = \lambda_n \sqrt{\frac{K_{\perp}}{-K_{\parallel}}} \approx \frac{\lambda_0}{n_n} \sqrt{\frac{n_c}{n(x)}}. \quad (9)$$

The location where $X_1 = \bar{\lambda}_{\perp}/16$ is indicated by an asterisk for each of the curves in Fig. 6. $\bar{\lambda}_{\perp}$ is the average perpendicular wavelength between $X = 0$ and $X = X_1$. The step model should be valid as long as the sheath thickness is less than approximately X_1^* ($\equiv \bar{\lambda}_{\perp}/16$), which is of the order of a millimeter. In PLT, the Debye length at the plasma edge can be conservatively estimated by taking $T_e \sim T_i < 100$ eV and $n_e > 10^{10} \text{ cm}^{-3}$, giving $\lambda_{De} < 0.07$ cm. The ion Larmor radius is estimated as $r_{Li} < 0.06$ cm, for $B_0 \sim 25$ kG. If the sheath thickness is of the order of the Debye length or the ion Larmor radius, then it approximately equals X_1^* for PLT parameters. Thus, the step model will probably be valid for PLT parameters.

For sheath thickness much greater than $\bar{\lambda}_1/16$, i.e., $X_1 \gg X_1^*$, the reflection coefficients approach those given by the ramp model. In Fig. 6, coupling is initially near optimum for $n_1/n_c = 10$. Increasing the ramp distance X_1 further will tend to make the coupling worse as conditions approach the case of coupling to a vacuum. The plasma is too overdense for optimum coupling for the cases where $n_1/n_c = 100$ and 1000. Decreasing the density gradient (increasing X_1) for these cases initially improves the coupling, before they also approach the vacuum case.

Finally, it is of interest to identify the regime where the ramp model is valid. Curve C in Fig. 1 is again used, but this time the density gradient remains fixed while the final density $n_1(\propto X_1)$ is varied. This model approaches the Brambilla model (curve A) as $X_1 \rightarrow \infty$. Reflected power R versus the distance X_1 is shown in Fig. 7, for $\Delta\phi = \pi/2$ and τ and $n = 10^{10}$ to 10^{13} cm^{-4} . After reaching a minimum reflection, R starts to increase with X_1 . The solution approaches an asymptotic value at large X_1 (the Brambilla solution) with a strongly damped oscillatory behavior. This behavior is due to the dependence of the phase of the reflected wave on the reflection location in the plasma. The Brambilla solution is approached when the density gradient no longer causes wave reflection. It is well-known that this is equivalent to satisfying the WKB solution,

$$\left| \frac{\frac{\partial k_{\perp}(x)}{\partial x}}{k_{\perp}^2} \right| = \alpha \ll 1.$$

For each curve in Fig. 1, we mark with an asterisk the point ($\equiv X_1^*$) where the WKB quantity α equals 0.2. These points correspond well with the location where the curves approach the Brambilla solution. The plasma beyond X_1^* does not contribute significantly to the waveguide coupling. The distance X_1^* becomes very short as the density gradient increases. For $\nabla n = 10^{13} \text{ cm}^{-4}$, for example, only the first few millimeters of plasma beyond the aperture contribute to the waveguide coupling. Therefore, for a plasma profile with a varying density gradient, the most important gradient is in the immediate vicinity of the waveguide aperture rather than that of the main plasma profile.

IV. Conclusion and Discussion

The dependence of the edge plasma profile on waveguide coupling has been quantitatively identified, both for the ramp (Brambilla) model and the step + ramp model. Typically, only the first few millimeters of the edge plasma is important. The predictions of linear coupling theory for lower hybrid waves are altered by including an overdense edge plasma in the plasma model. Coupling is found to depend strongly on

the edge density as well as density gradient. The regimes, where one or the other of these parameters is most important, have been investigated. The model of a density step plus a density ramp should be applicable for expected tokamak parameters.

The major implications of the problem of coupling to an overdense plasma can be derived from the simple impedance matching argument contained in Equations (5) and (7). In general, coupling is optimized when the edge density satisfies $n_o/n_c \approx n_m^2$. An overdense plasma at the coupler aperture is advantageous, because it reduces the reactive component of the plasma impedance and thus reduces reflected power for a well defined spectrum. An overdense edge plasma is also favorable from the point of view of reducing ponderomotive effects of the guide aperture [11,14]. These effects depend on the parameter $E_o^2/n_o k_B T$, which is reduced for larger values of n_o .

Acknowledgments

We thank Drs. W. M. Hooke, R. W. Motley, and S. Bernabei for their encouragement and suggestions.

This work was supported by the U.S. Department of Energy Contract No. DE-AC02-76-CHO3073.

REFERENCES

- [1] LALLIA, P., Proc. Second Topical Conf. on RF Plasma Heating, Lubbock, Texas, paper C-3 (1974).
- [2] BRAMBILLA, M., Nucl. Fusion 16 (1976) 47.
- [3] BERNABEI, S., HEALD, M. A., HOOKE, W. M., MOTLEY, R. W., PAOLONI, F. J., BRAMBILLA, M., and GETTY, W. D., Nucl. Fusion 17 (1977) 929.
- [4] PARKER, R. R., Massachusetts Institute of Technology QPR No. 102 (1971) 97.
- [5] PACHER, H. D., Max. Planck Institute fur Plasma Physik, IPP 2/247 (1979).
- [6] KRAPCHEV, V., and BERS, A., Nucl. Fusion 18 (1978) 519.
- [7] BOLEY, C. D., ANL/FPP/TM-135, June 1980.
- [8] BARNES, C. W., COHEN, S. A., and DYLLA, H. F., "Langmuir Probe Measurements of the Scrape-Off Plasma in PLT," Status of Ohmic Heating in PLT, 7-8 September 1977 (unpublished). Bull. Am. Phys. Soc. 22 (9) (October 1977)
- [9] HORTON R., WONG, K. L., ONO, M., WILSON, J. R., and FISCH, N., Bull. Am. Phys. Soc. 24 (1979) 957.
- [10] FUKUYAMA, A., MORISHITA, T., and FURUTANI, Y., Plasma Physics 22 (1980) 565.
- [11] WILSON, J. R., Ph.D. Thesis, Princeton University (1980).
- [12] GOLANT, V. E., Zh. Tekh. Fiz. 41 (1971) 2492 [JETP 16 1980 (1972)].

- [13] MOTLEY, R. W., Phys. Fluids 23 (1980) 2061.
- [14] MORALES, G. J., Phys. Fluids 20 (1977) 1164.

81X0062

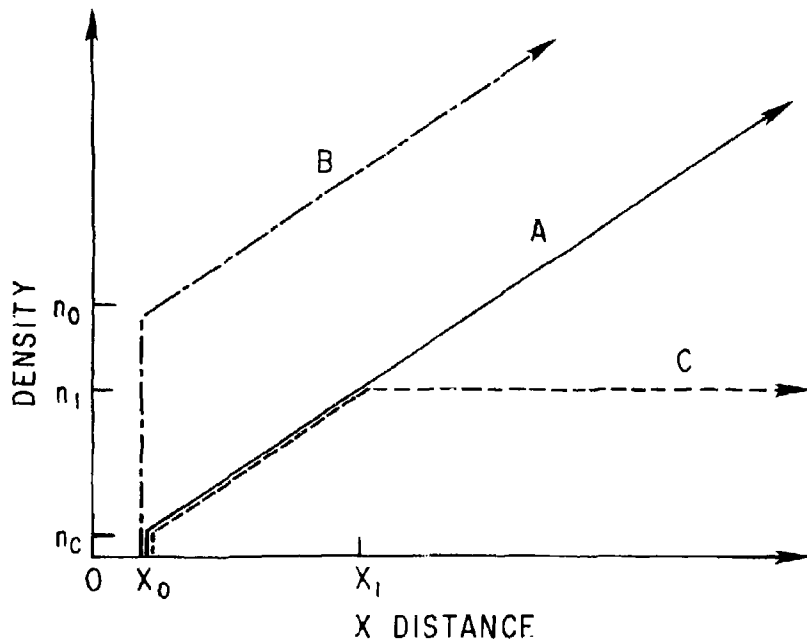


Fig. 1. Model edge density profiles, showing ramp (A), step plus ramp (B), and ramp plus plateau (C).

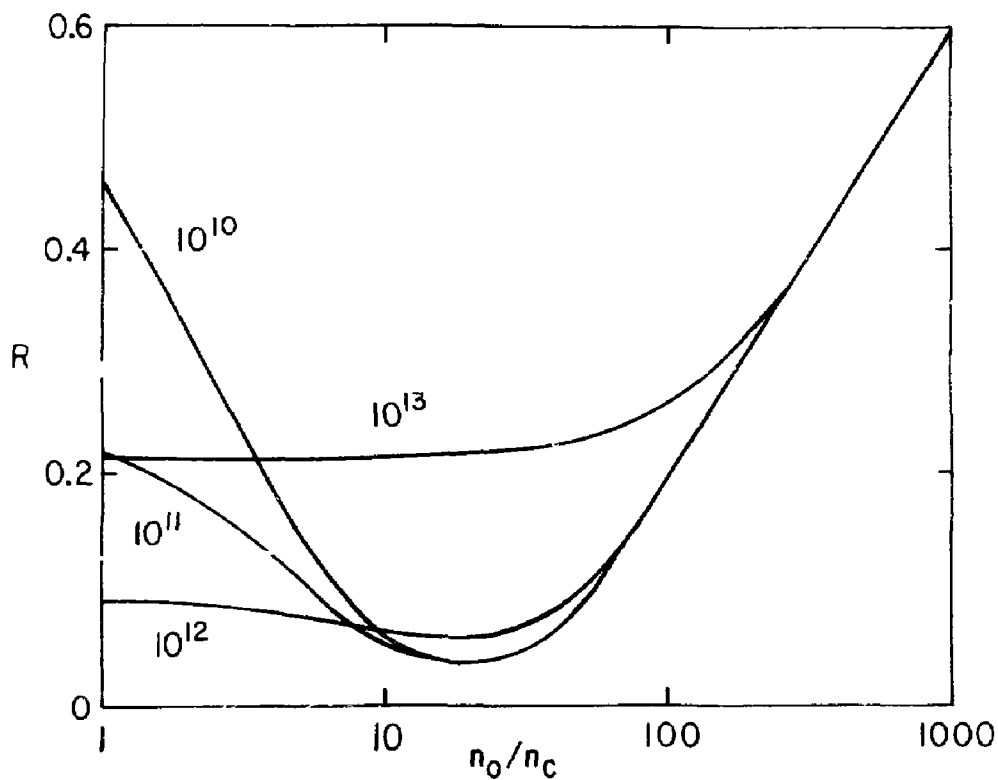


Fig. 2. Reflected power versus edge density, for density gradients of 10^{10} to 10^{13} cm⁻⁴ and phasing between the guides of π . (PPPL-809017)

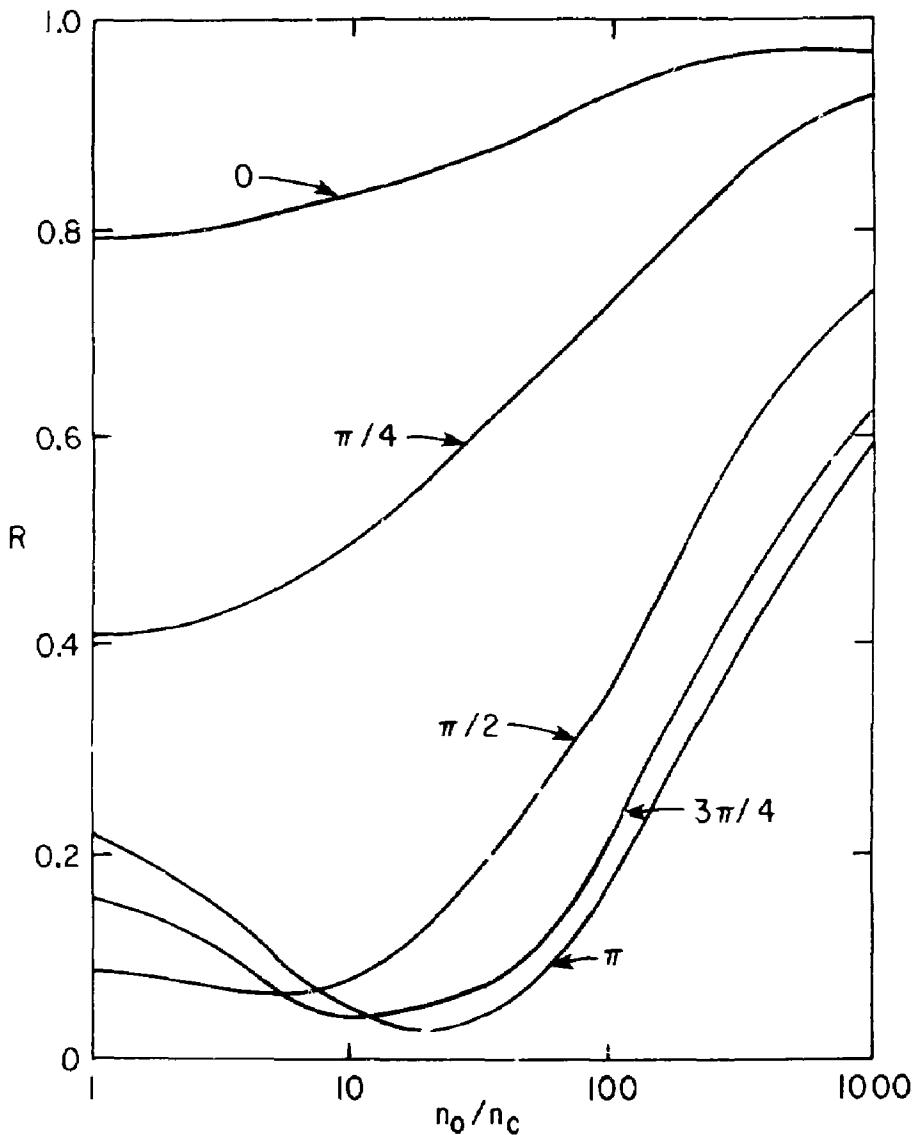


Fig. 3. Reflected power versus edge density, for phasings between the guides of 0, $\pi/4$, $\pi/2$, $3\pi/4$, and π . (PPPL-809020)

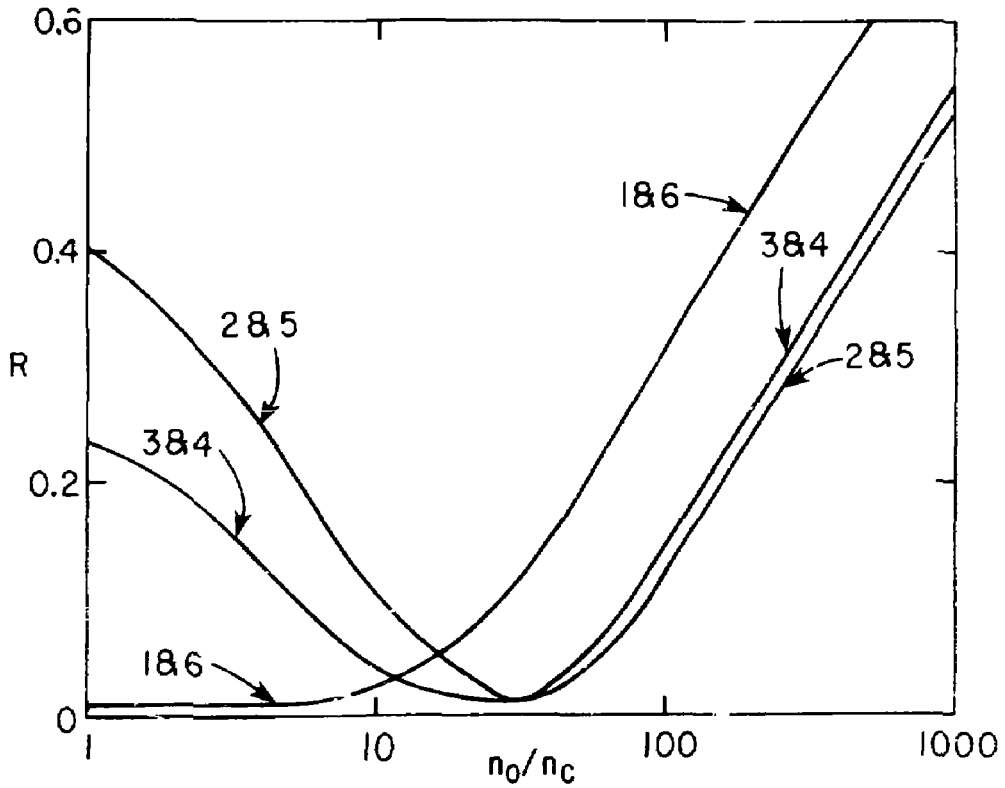


Fig. 4. Reflected power in the individual guides versus edge density, for phasing between the guides of π . (PPPL-809018)

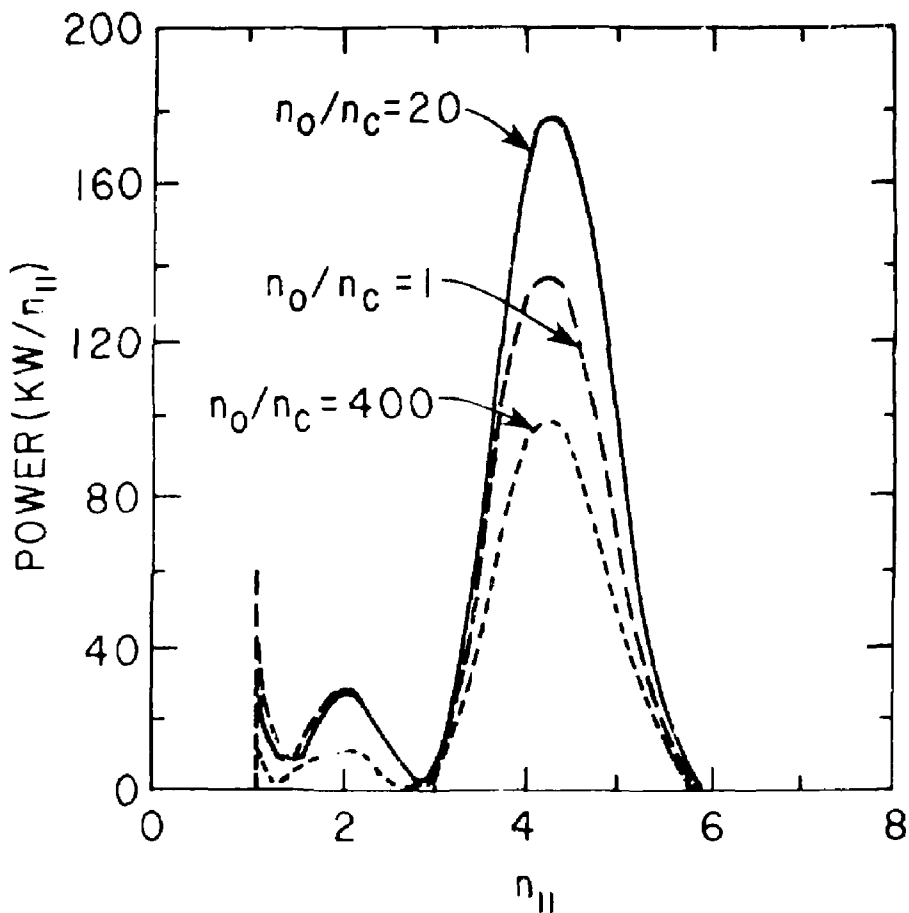


Fig. 5. Spectral density of radiated power versus parallel index of refraction, for normalized edge densities of 1, 20, and 400 and phasing between the guides of π . (PPPL-809021)

81X0063

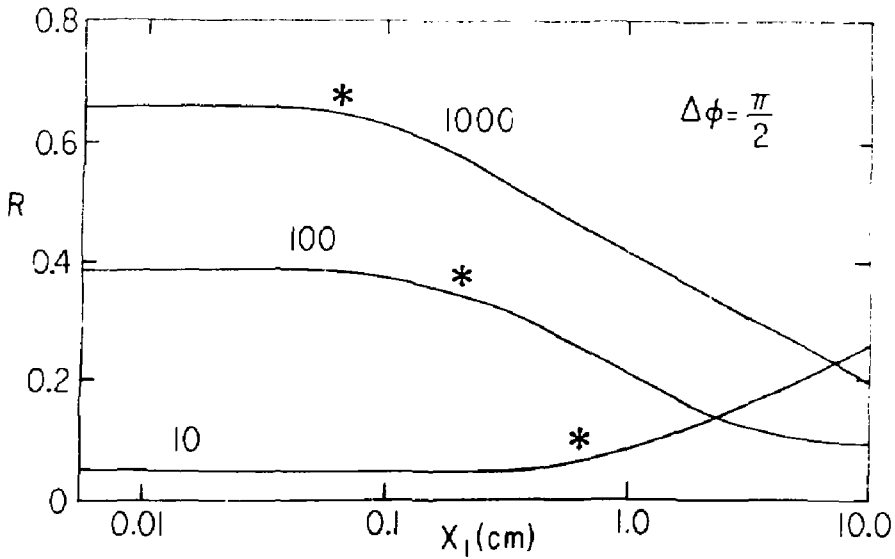
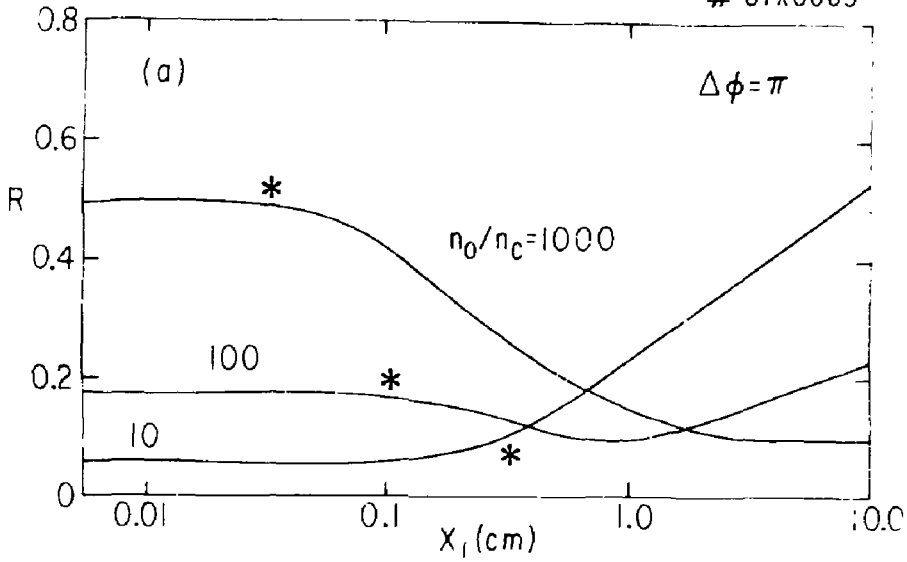


Fig. 6. (a) Reflected power versus ramp distance X_1 (Fig. 1, curve C), for normalized plateau densities of 10, 100, and 1000, and phasing between the guides of π . (b) Same as (a), with phasing between the guides of $\pi/2$.

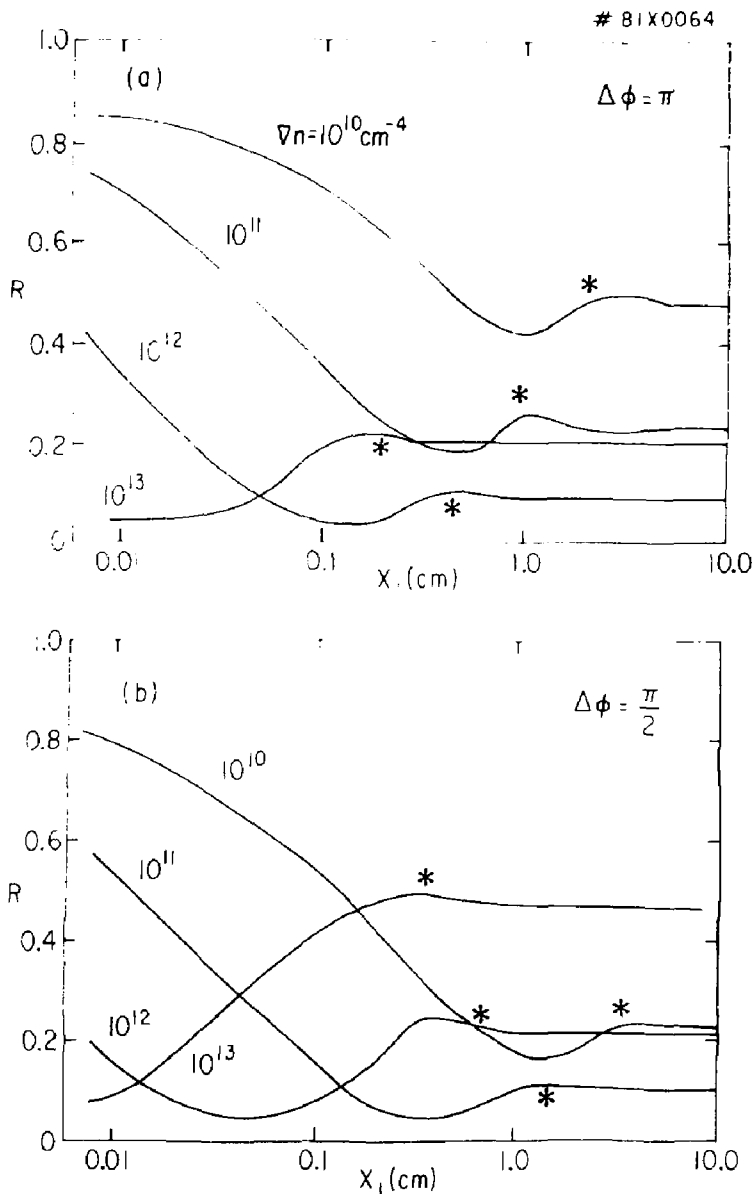


Fig. 7. (a) Reflected power versus ramp distance X_1 (See Fig. 1, curve C), for density gradients of 10^{10} to 10^{13} cm^{-4} , and phasing between the guides of π . (b) Same as (a), with phasing between the guides of $\pi/2$.